Study of oligomerization of human β_2 microglobulin

Ajit Kumar Sahoo

A dissertation submitted for the partial fulfilment of BS-MS dual degree in Science

Indian Institute of Science Education and Research Mohali

May 2020

Certificate of Examination

This is to certify that the dissertation titled "Study of oligomerization of human β_2-microglobulin" submitted by Mr. Ajit Kumar Sahoo (Reg.No. MS15158) for the partial fulfilment of BS-MS dual degree programme of the Institute, has been examined by the thesis committee duly appointed by the Institute. The committee finds the work done by the candidate satisfactory and recommends that the report be accepted.

Dr. Rajesh Ramachandran **Dr. Indrajit Lahiri** **Dr. Purnananda Guptasarma (Supervisor)**

Dated: May 04, 2020

Declaration

The work presented in this dissertation has been carried out by me under the guidance of Dr. Purnananda Guptasarma at the Indian Institute of Science Education and Research Mohali.

This work has not been submitted in part or in full for a degree, a diploma, or a fellowship to any other university or institute. Whenever contributions of others are involved, every effort is made to indicate this clearly, with due acknowledgement of collaborative research and discussions. This thesis is a bona fide record of original work done by me, and all sources listed within have been detailed in the bibliography.

Ajit Kumar Sahoo
(Candidate)

Dated: May 04, 2020

In my capacity as the supervisor of the candidate's project work, I certify that the above statements by the candidate are true to the best of my knowledge.

Dr. Purnananda Guptasarma
(Supervisor)

ACKNOWLEDGEMENT

I duly acknowledge the efforts put in by the faculty members of IISER Mohali, who have guided and helped me in the course of the last five years.

I am immensely grateful to Dr. Purnananda Guptasarma for accepting me as his Master's thesis student. Through his courses, his valuable life lessons, feedbacks and discussions in the lab, the anecdotal narrations, and his sense of humor, he has inspired me to be a thorough academician, professional, and humble person. He truly is a great mentor.

This project would have been impossible without the constant support and encouragement of PG lab members. I am extremely thankful to Ms. Arpita Sarkar for her undying patience, generous encouragement, and her guidance for mastering the techniques in the lab. She has been a constant support during my cloning failures. Every time I have given up, she has motivated me with some new troubleshooting ideas. I would also like to thank Ms. Arpita Mrigwani, for being the most caring senior and always present there whenever I need her. A special thanks to Mr. Archit Gupta for brainstorming with me and helping me to carry out some of my experiments and entertaining the lab with his sense of humor. Dr. Neeraj Dhaunta, Dr. Bhishem Thakur, Ms. Harman Kaur, Ms. Snehal Waghmare have constantly motivated me and have kept the ambience in the lab cheerful. I also thank Dr. Rajesh Ramachandran and Dr. Indrajit Lahiri for reviewing this report and providing helpful inputs.

To a great extent, I thank my parents, brother, and friends for their unconditional support and constant motivation. Finally, I would like to thank DBS, IISER Mohali, and INSPIRE-DST for facilities and financial support.

List of Figures

List of Tables

Notation

β_2m - β_2 microglobulin

DRA - Dialysis Related Amyloidosis

ANS - 8-anilino-1-naphthalenesulfonic acid

LLPS - Liquid-liquid phase separation

MHC - Major histocompatibility complex

Ni-NTA - Nickel-Nitrilotriacetic acid

SDS-PAGE - Sodium dodecyl sulfate–polyacrylamide gel electrophoresis

R - Reducing SDS-PAGE sample loading buffer

N.R - Non-reducing SDS-PAGE sample loading buffer

L or M - Protein ladder or Marker

Contents

Abstract

We found β_2 microglobulin (β_2m), the causative protein of Dialysis Related Amyloidosis (DRA), forms oligomers when it was loaded with non-reducing sample loading buffer in an SDS-PAGE. Upon treating the sample with reducing sample loading buffer, these oligomers dissociated into monomers, indicating that the intermolecular disulfide bonds might be responsible for its oligomerization. This result was confirmed by further experiments with di-cysteine mutants, which, as anticipated, didn't show any oligomerization. We have hypothesised that due to the burial of cysteines in β_2m's native structure, we were not able to observe any higher-order oligomers. Hence, in order to enhance the propensity of formation of the intermolecular disulfide bonds, we decided to carry out the purification under denaturing conditions (with 8M urea), so as to expose the buried cysteines. As expected, we found a profound increment in intensity and the number of higher-order oligomers, which, we propose, could be used as a protein ladder (for SDS PAGE). We next thought to enrich these higher-order oligomers by crosslinking the lower order oligomers with glutaraldehyde, which would lock the formed oligomers and drive the equilibrium towards more populated lower-order oligomers, which in turn increase the probability of molecular collision between them to form more higher-order structures. Surprisingly, we found that glutaraldehyde was not able to crosslink β_2 microglobulin. Further, we tracked the formation of these oligomers during the denaturing purification and found that they are forming just after the lysis of the cell.

In a different study, our lab has shown that β_2 microglobulin forms amorphous aggregates in presence of Ca^{2+}, which, if incubated for 3-4 weeks, gets converted into amyloid aggregates. In order to check if Ca^{2+} is enhancing these disulfide-linked oligomers, we loaded these Ca^{2+} induced amorphous aggregates with non-reducing sample loading buffer in an SDS-PAGE. However, the SDS-PAGE revealed a single band corresponding to monomer, indicating a totally different nature of these Ca^{2+} induced oligomers. In order to further characterize these Ca^{2+} induced oligomers, we monitored intrinsic tryptophan fluorescence, ANS binding, and intrinsic blue fluorescence, both in presence and absence of Ca^{2+}. We have been able to show the exposure of some hydrophobic patches upon Ca^{2+} binding, which we propose to be the

initial driver of Ca^{2+} induced β_2m self-assembly. Additionally, to check if β_2 microglobulin phase separates into liquid condensates on its pathway to amorphous aggregates, we performed confocal imaging just after the addition of Ca^{2+}, which showed mesh-like networks eliminating Liquid-Liquid Phase Separation (LLPS) of β_2m.

Chapter 1

1.1 Introduction

1.1.1 Major Histocompatibility Complex

Major histocompatibility complex is displayed on the surface of human cells, which helps the immune system to recognize foreign particles. It is divided into two types: Class-I and Class-II. Class-I helps in recognizing endogenous antigens that originate from the cytoplasm, whereas class-II helps in recognizing exogenous antigens.

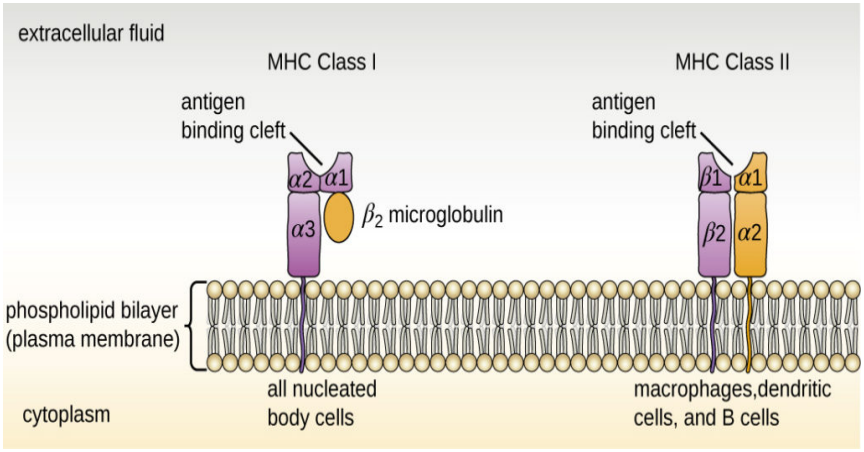

Figure 1 : Types of major histocompatibility complex
Adapted from lumenlearning.com (Major Histocompatibility Complexes and Antigen-Presenting Cells , n.d.)

1.1.2 β_2 microglobulin and its role in Dialysis Related Amyloidosis

β_2 microglobulin (β_2m) is a light chain of class-I Major Histocompatibility Complex (MHC-I). It is a small 99 residue protein, noncovalently attached to the cell membrane.

It contains seven antiparallel β strands with β-sandwich fold. Among seven β strands, strand B and E have the highest aggregation propensity (Le Marchand, et al., 2018). β strand B is inter-connected with strand F via an intramolecular disulfide bond, preventing itself from unleashing its aggregation potential, whereas strand E has some hydrophobic patches, buried in its native structure.

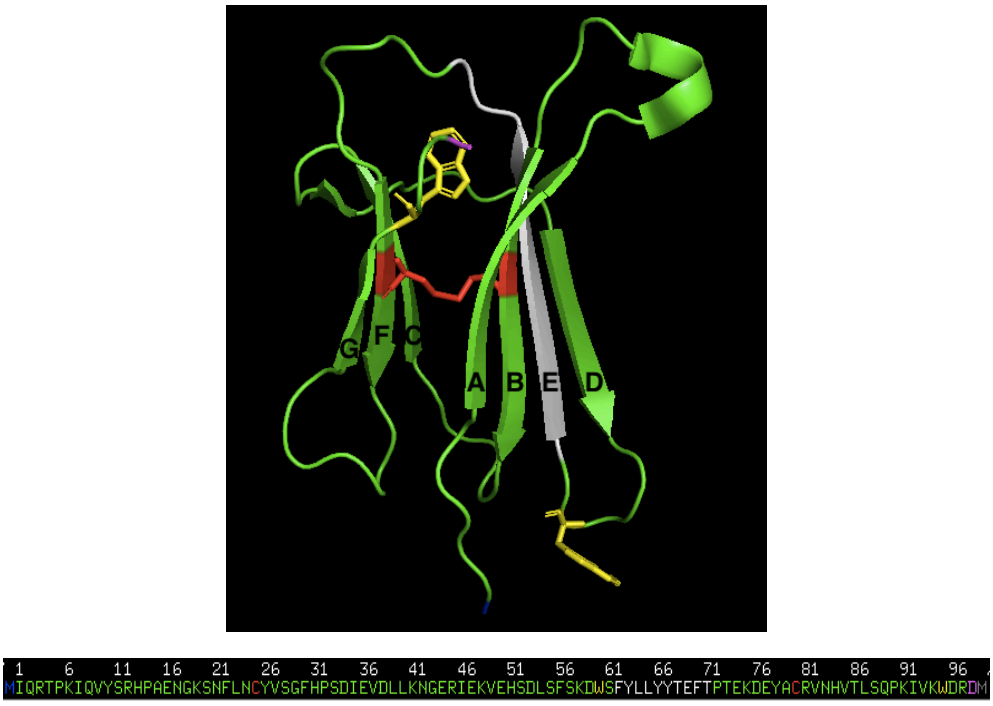

Figure 2 : Structure (top) and sequence (bottom) of β_2 microglobulin
Drawn using pymol (PDB ID: 2YXF)
Here, Blue colour denotes N terminal, Yellow, red, and grey colour represent tryptophan residues, cysteines with disulfide bond, and hydrophobic patches respectively.

During natural turnover, when the MHC-I complex is disassembled, the non-covalently attached β_2 microglobulin is thought to be simply shed into extracellular fluids by the displaying cells, while the membrane-tethered HLA (also known as α) chain is internalized. It is then carried to the kidney where it is degraded in the proximal tubules (Floege J, 1991) (Floege J K. M., 2001). As a result, β_2 microglobulin is always present in an equilibrium concentration of 1-3 ug/ml in the serum of healthy individuals. In patients suffering from renal dysfunction, the degradation of β_2 microglobulin is disrupted (Miyata T, 1998), which results in a 25-60 fold increase in β_2m concentration

in the blood (Floege J K. M., 2001). As a consequence, β_2m tends to form amyloid aggregates and deposits in the joints of patients receiving hemodialysis-based treatments and causes carpal tunnel syndrome, amyloid arthropathy and pathological bone disruption, which is collectively known as Dialysis Related Amyloidosis (DRA) (Drueke, 1998) (Radford SE, 2005).

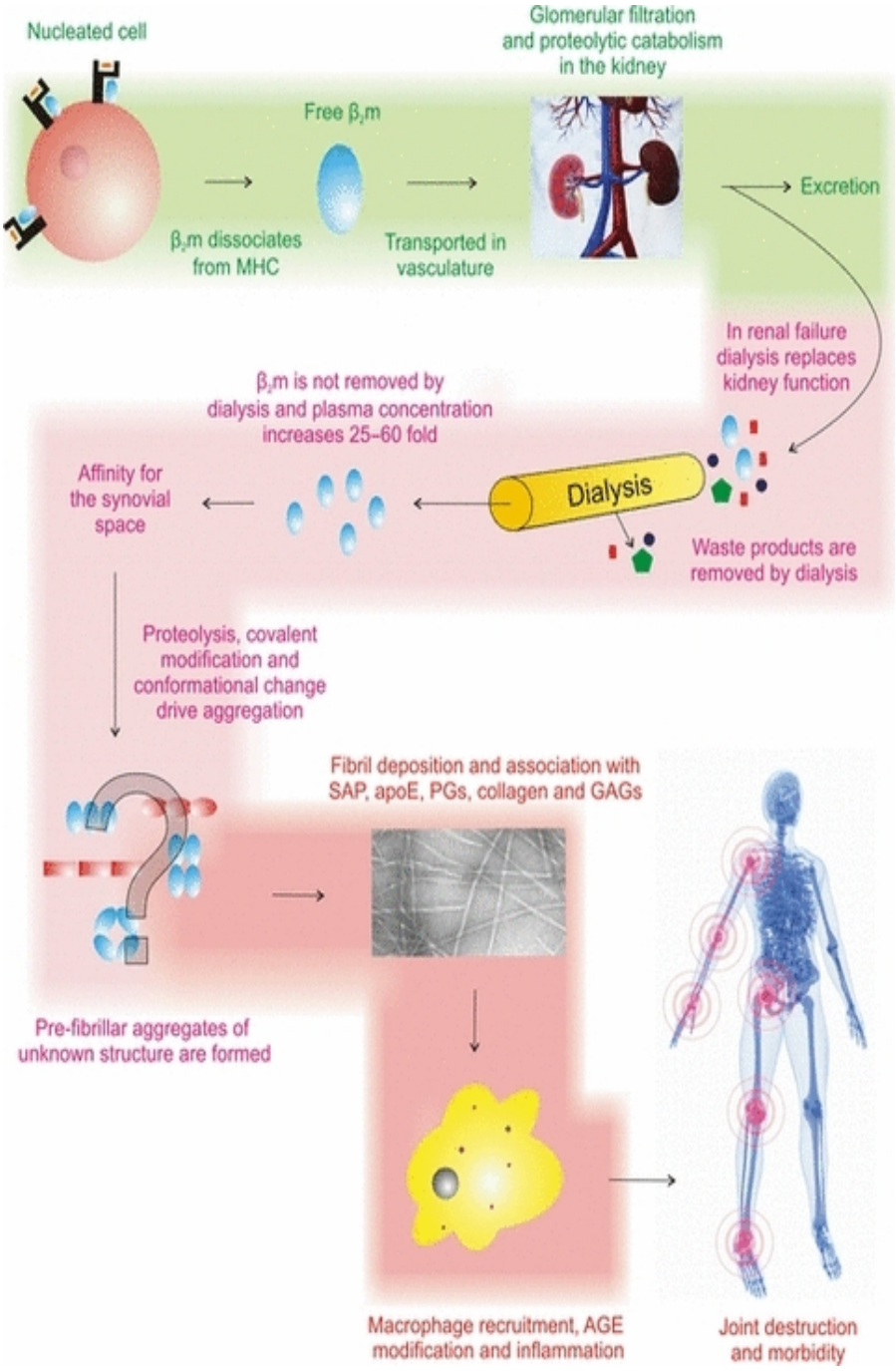

Figure 3 : Schematic of the key processes which result in the pathological symptoms experienced in DRA (Eichner T, 2011)

However, β_2m, as a protein, is exceptionally soluble in aqueous solution at physiological pH and ionic strength. In fact, it can be concentrated up to millimolar concentration and incubated for months at 37 °C with no consequent aggregation or precipitation (Radford SE, 2005) (McParland VJ, 2000) (Myers SL, 2006) (Verdone G, 2002). Thus, a High concentration of β_2m, found in DRA patients, alone can't explain its aggregation and deposition.

It is not even as if the structural differences between soluble β_2m and HLA bound β_2m reveal very significant clues to its aggregation because both of them show very similar structures with minute differences in β strand composition and arrangement (Radford SE, 2005). Also, β_2m shows the highest structural stability at physiological pH (Eichner T, 2011), the pH at which it aggregates in the serum. Thus, the precipitation and deposition of β_2m at pH 7.4 continues to perplex those studying DRA.

In 2001, Miranker and colleagues reported that Cu^{2+}, a divalent ion, binds to β_2m specifically, and promotes its oligomerization and amyloid formation (Calabrese MF, 2008) (Morgan CJ, 2001). Although Cu^{2+} is present at vanishingly low concentration in the human body, it has been suggested that the copper present in the equipment used for dialysis might increase its concentration in the serum leading to oligomerization, aggregation, and precipitation of β_2m (Calabrese MF, 2008). However, this is yet to be established equivocally (Hodkinson JP, 2012).

In the meantime, Guptasarma and colleagues have shown that Ca^{2+}, a physiologically relevant divalent ion, can bind to β_2m at physiological pH and causes conformational changes, which promote its precipitation into amorphous aggregates that subsequently transform into amyloid aggregates (Kumar S., 2014). Here, we tried to characterize Ca^{2+} induced oligomers using intrinsic tryptophan fluorescence, ANS binding, and blue fluorescence. We showed, upon Ca^{2+} binding, some hydrophobic patches of β_2m is getting exposed. So, we propose that β strand E, being the most hydrophobic and

present close to a predicted Ca^{2+} binding site EKD (74-76) (Kumar S., 2014), shows some dynamics upon binding to Ca^{2+}, which initiates Ca^{2+} induced self-assembly of β_2m. In a different study, we also made a potential SDS-PAGE ladder, exploiting the intermolecular disulfide bond-forming capability of β_2m.

1.2 Materials

1.2.1 Plastic wares and chemicals:

Plastic and glasswares were purchased from Thermo Scientific®; Falcon®, USA; Tarsons®, India; Fisher Scientific®, USA. Bacterial media, agar, salts, and buffers were purchased from HiMedia®, France. Chemicals were procured from Merck limited®, USA.

1.2.2 Constructs:

The human wild type β_2 microglobulin in pET 23a plasmid was gifted by Neeraj Dhaunta (Indian Institute of Science Education and Research, Mohali).

1.3 Methods:

1.3.1 Preparation of competent cells

A single bacterial colony of BL21 (DE3) pLysis Star cells were taken from a culture plate and incubated in 10 ml LB media overnight at 37 °C. 100 µl of this primary culture was taken and incubated in 100 ml LB media till the optical density of the culture reached 0.4 - 0.6. To pellet down the cells, the culture was centrifuged for 15 minutes at 6000 rpm at 4 °C. The pellet was resuspended in 10 ml of 0.1 M ice-cold $CaCl_2$ solution and kept on ice for 15 min. Subsequently, the solution was centrifuged at 6000 rpm at 4 °C for 15 min. The supernatant was discarded, and then the pellet was resuspended in 5 ml of 0.05 M $CaCl_2$ solution and incubated on ice for 45 min. The cell recovery was made by spinning down the solution at 2000 rpm at 4 °C for 5 min. The pellet obtained was finally resuspended in 85 % 0.1 M $CaCl_2$ solution and 15 % glycerol. Aliquots of 100 µl were made and stored at -80 °C.

1.3.2 Transformation

The competent cells were thawed on ice for 10 minutes. 1 µg DNA was added and incubated on ice for 30 min. Heat shock was given at 42 °C for 90 seconds, and the cells were transferred back on ice for 5 min. Subsequently, 1 ml LB media was added and the culture was incubated at 37 °C for an hour in a water bath. The Media was then centrifuged at 5000 rpm for 5 min. The pellet was resuspended in 200 µl LB media and plated on antibiotic-containing LB agar plates.

1.3.3 Plasmid isolation

1. 5 mL of culture was centrifuged at 13400 rpm for 2 min at RT
2. The supernatant was discarded, and the pellet was dissolved in 100 µL of autoclaved MQ.
3. 100 µL of freshly prepared lysis buffer was added and gently tapped. For 1 mL of lysis buffer, add 50 µL of 20% SDS solution, 20 µL of 0.5 M EDTA and 10 µL of 10 N NaOH in 910 µL of water.
4. The samples were boiled at 100 °C for 2 minutes (until the solution becomes clear).

5. 50 µL of 0.5 M MgCl2 was added. Tapped and kept on ice for 2 minutes. For 100 mL, 60 mL of potassium acetate, 11.5 mL glacial acetic acid, and 28.5 mL H_2O were mixed. Stored at 4 °C.
6. Immediately tapped and centrifuged at 13400 rpm for 2 min, RT.
7. The supernatant was transferred into another MCT containing 600 µL of Isopropanol.
8. Kept on ice for 5 min.
9. Centrifuged at 13400 rpm for 2 min, RT.
10. 70% ethanol wash and the pellet was dried completely
11. Pellet was dissolved in 50 µL of autoclaved MQ.
12. Stored at -20 °C.

1.3.4 β_2m expression

A clone of wildtype human β_2m with a C-terminal 6xHis tag, sub-cloned in the pET 23a vector, was overexpressed in and purified from the BL21 Star (DE3) pLysS strain. The transformed cells were grown at 37 °C overnight with 100 µg/ml ampicillin and 35 µg/ml chloramphenicol. The primary culture was then sub-cultured into 500 ml of LB broth in a 1.0-liter flask containing the same antibiotics and was grown in a rotary shaker at 37 °C, until it reached an OD600 of 0.6. Then protein expression was induced with 1 mM IPTG and grown again for 6 hrs. Cells were then pelleted through centrifugation at 8000 rpm for 10 minutes and treated as given below.

1.3.5 β_2m purification under denaturing conditions and on-column refolding

Pelleted cells containing overexpressed β_2m were then re-suspended in 100 mM NaH_2PO_4, 10 mM Tris-Cl, 8 M urea, pH 8 (70 µl per ml of culture), and sonicated. Then it was centrifuged at 10000 rpm for 72 mins at 10 °C to separate out the cellular debris. The supernatant was then loaded onto a Qiagen Ni-NTA affinity column (1 ml resin) pre-equilibrated with the sonication buffer. Non-specifically bound proteins were then removed by washing with 20 ml of wash buffer (100 mM NaH_2PO_4, 10 mM Tris-Cl, 8 M urea, pH 6.5). The bound 6xHis tagged β_2m was then eluted using standard elution buffer (100 mM NaH_2PO_4, 10 mM Tris-Cl, 8 M urea, pH 4.5) and stored at 4 °C. We couldn't refold the protein. For on-column refolding purification, 5 washes were given with a,b,c,d,e (in respective order).

a. 100 mM NaH_2PO_4, 10 mM Tris-Cl, 4 M urea, 40 mM imidazole, pH 8.0

b. 100 mM NaH_2PO_4, 10 mM Tris-Cl, 2 M urea, 40 mM imidazole, pH 8.0

c. 100 mM NaH_2PO_4, 10 mM Tris-Cl, 1 M urea, 40 mM imidazole, pH 8.0

d. 100 mM NaH_2PO_4, 10 mM Tris-Cl, 0.5 M urea, 40 mM imidazole, pH 8.0

e. 100 mM NaH_2PO_4, 10 mM Tris-Cl, 40 mM imidazole, pH 8.0.

Then it was eluted with 100 mM NaH_2PO_4, 10 mM Tris-Cl, 250 mM imidazole, pH 8.0. It was then dialysed against de-ionized water using 3 kDa dialysis membrane and stored at 4 °C.

1.3.6 β_2m purification under Native conditions

Pelleted cells containing overexpressed β_2m were then re-suspended in 50 mM NaH_2PO_4, pH 8.0, 0.5 M NaCl (70 µl per ml of culture), and sonicated. Then it was centrifuged at 10000 rpm for 72 mins at 10 °C to separate out the cellular debris. The supernatant was then loaded onto a Qiagen Ni-NTA affinity column (1 ml resin) pre-equilibrated with the sonication buffer. Non-specifically bound proteins were then removed by washing with 20 ml of wash buffer (50 mM NaH_2PO_4, pH 8.0, 0.5 M NaCl, 40 mM imidazole). The bound 6xHis tagged β2m was then eluted using standard elution buffer (50 mM NaH_2PO_4, pH 8.0, 0.5 M NaCl, 250 mM imidazole). It was then dialysed against de-ionized water using 3 kDa dialysis membrane and stored at 4 °C.

1.3.7 SDS-PAGE

All SDS-PAGE experiments were done with 15 % Lower and 5 % upper gel. The protocol for 15 % Lower (left) and 5 % upper gel (right) is given below. For glutaraldehyde cross-linking studies, samples were incubated for 30 minutes with glutaraldehyde before loaded in the SDS-PAGE.

Table 1: SDS-PAGE gel composition

Water	2.4 ml
Lower tris(includes SDS)	2.5 ml
Acrylamide	5 ml
APS	50 µl
TEMED	10 µl

Water	1.167 ml
Upper tris(includes SDS)	0.5 ml
Acrylamide	0.333 ml
APS	12.5 µl
TEMED	5 µl

1.3.8 Agarose gel electrophoresis

For 1 % agarose gel, 1 gm of agarose was added to 100 ml of TAE buffer and was heated in the microwave. Then 1 µl EtBr was added, and the gel was cast.

1.3.9 Intrinsic tryptophan fluorescence

Steady-state fluorescence measurements were carried out at room temperature (24 ± 1 °C) on a Cary Eclipse Fluorescence Spectrophotometer. For this study 51 µM β_2m was incubated with 50 mM $CaCl_2$ for 1 hr. The samples were excited at 295 nm and spectra were collected over the range of 320–400 nm. The obtained spectra were averaged over five scans. The path length of the cuvette was 3 mm.

1.3.10 ANS binding

Steady-state fluorescence measurements were carried out at room temperature (24 ± 1 °C) on a Cary Eclipse Fluorescence Spectrophotometer. For this study 51 µM β_2m was incubated with 50 mM $CaCl_2$ and 10 µM ANS for 1 hr. The samples were excited at 350 nm, and spectra were collected over the range of 400–550 nm. The obtained spectra were averaged over five scans. The path length of the cuvette was 3 mm.

1.3.11 Intrinsic Blue fluorescence

Steady-state fluorescence measurements were carried out at room temperature (24 ± 1 °C) on a Cary Eclipse Fluorescence Spectrophotometer. For this study 51 µM β_2m was incubated with 50 mM $CaCl_2$ for 1 hr. The samples were excited at 310 nm and, spectra were collected over the range of 360–500 nm. The obtained spectra were averaged over five scans. The path length of the cuvette was 3 mm.

1.3.12 Confocal microscopy

β_2m was labelled with FITC as per the protocol from sigma. A mixer of 20 µM β_2m (including 1% FITC labelled), 50 mM $CaCl_2$ and 2 % PEG was made. A small drop of this mixer was put on a glass slide (covered with a coverslip) and imaged on a confocal microscope.

1.3.13 Cloning of di-cysteine mutant

In order to create a di-cysteine mutant by SOE PCR following primers were ordered from sigma.

β_2m EF	TTATAACATATGATCCAGCGTACTCCAAAG
β_2m C1F	GAATTCTTATGTGTCTGGGTTTCATCC
β_2m C1R	ACCCAGACACATAAGAATTCAGGAAATTTGAC
β_2m C2F	ATGCCTCTCGTGTGAACCATGTGAC
β_2m C2R	ACATGGTTCACACGAGAGGCATACTCATC
β_2m ER	ATATATCTCGAGCATGTCACGATCCCAC

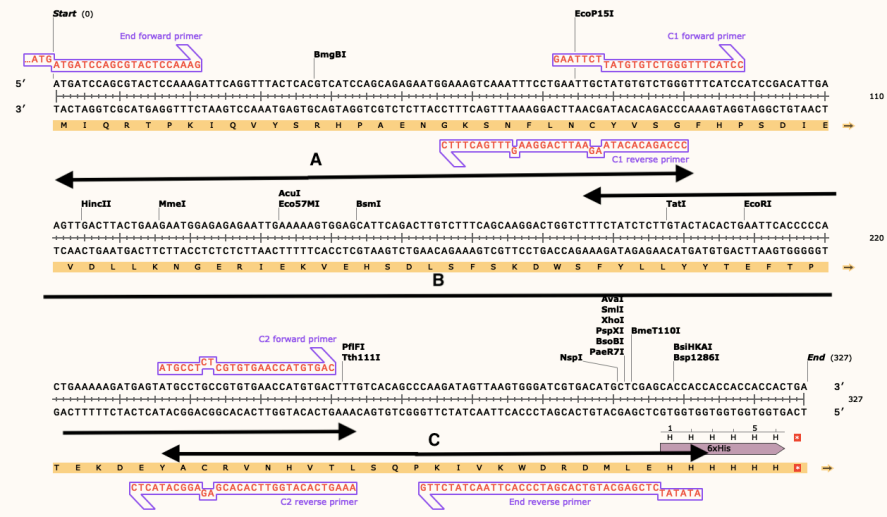

Figure 4 : Schematic diagram of the fragments and primers used for SOE PCR
Drawn using Snapgene software

Using the following PCR protocols, three fragments were synthesized (Figure 4 and 5). Then a step-down PCR was performed for the synthesis of A+B+C fragment (Figure 6). The amplicons of the final gene construct were then extracted from the gel using Qiagen's kit for Gel Extraction. They were then digested with *Nde I* and *Xho I* at 37 °C for 2 hrs. After the digestion, they were purified using Qiagen's kit for PCR product purification. Another pET23a vector containing an insert of 1.6 kb length was also digested with *Nde I* and *Xho I* at 37 °C for 2 hrs. Digested products were run in a 1% agarose gel, and the double-cut pET23a vector was extracted from the gel following the standard protocol of Qiagen's kit for Gel Extraction. To this double cut pET23a vector, PCR purified products were added, and the whole mixer was incubated with the appropriate volume of 1X T4 ligase buffer and T4 ligase (following the instructions of T4 ligase protocol, Table 8) at 25 °C for 3hrs. The ligation mixer was then transformed into the XL1 Blue cells and plated on ampicillin and tetracycline plates. On the next day, few colonies were observed on the plates. Few of these colonies were further verified to be positive through Colony PCR (Figure 7). We proceeded with one of these tentatively positive colony and performed double digestion with *Nde I* and *Xho I* at 37 °C for 2 hrs . Thus, we verified that the colony selected was positive and had the proper gene construct. A primary culture was inoculated with this colony. The plasmid was then isolated and given for sequencing (Figure 8 and 9). Further, we transformed the plasmid into Bl21 (DE3) pLysS star cells for over expression of the protein of interest. Note: All the volumes, mentioned below, may vary depending on the stock concentrations.

Table 2: PCR reaction mixer (left) and parameters (right) for fragment A

Template (Plasmid)	0.2 µl
5 X vegapol buffer	4.0 µl
β2M EF	0.5 µl
β2M C1R	0.5 µl
Vegapol	0.2 µl
dNTPs	0.5 µl
dH_2O	14.1 µl

Temperature	Time
95 °C	3 minutes
95 °C	30 seconds
62 °C	45 seconds
72 °C	40 seconds
72 °C	10 minutes

Table 3: PCR reaction mixer (left) and parameters (right) for fragment B

Template (Plasmid)	0.2 µl
5 X vegapol buffer	4.0 µl
β2M C1F	0.5 µl
β2M C2R	0.5 µl
Vegapol	0.2 µl
dNTPs	0.5 µl
dH_2O	14.1 µl

Temperature	Time
95 °C	3 minutes
95 °C	30 seconds
62 °C	45 seconds
72 °C	40 seconds
72 °C	10 minutes

Table 4: PCR reaction mixer (left) and parameters (right) for fragment C

Template (Plasmid)	0.2 µl
5 X vegapol buffer	4.0 µl
β2M C2F	0.5 µl
β2M ER	0.5 µl
Vegapol	0.2 µl
dNTPs	0.5 µl
dH_2O	14.1 µl

Temperature	Time
95 °C	3 minutes
95 °C	30 seconds
66 °C	45 seconds
72 °C	40 seconds
72 °C	10 minutes

Table 5: PCR reaction mixer (left) and parameters (right) for fragment A+B+C

5 X vegapol buffer	4.0 µl
Template A	2 µl
Template B	1µl
Template C	2.5 µl
Vegapol	0.2 µl
dNTPs	0.5 µl
dH_2O	9.8 µl

Temperature	Time
95 °C	3 minutes
95 °C	30 seconds
65 °C	20 seconds
60 °C	20 seconds
55 °C	20 seconds
72 °C	40 seconds
72 °C	10 minutes

Table 6: PCR reaction mixer (left) and parameters (right) for Colony PCR

Template (a colony) + dH_2O	12.7 µl
5 X flexi buffer	4.0 µl
T7F	1 µl
T7R	1µl
Flexi DNA polymerase enzyme	0.1 µl
dNTPs	0.2 µl
$MgCl_2$	1 µl

Temperature	Time
95 °C	5 minutes
95 °C	30 seconds
55 °C	55 seconds
72 °C	30 seconds (2min for +ve control)
72 °C	10 minutes

Table 7: Reaction mixer for restriction digestion

Template	15.0 µl
Ndel I	1.5 µl
Xho I	1.5 µl
F.D. buffer	6.0 µl
dH_2O	36.0 µl

Table 8: Reaction mixer for ligation (Vector : Insert = 1 : 5)

Vector	7.7 µl
Insert	1.4 µl
10 X ligase buffer	1.1 µl
Ligase	0.4 µl
dH_2O	0.4 µl

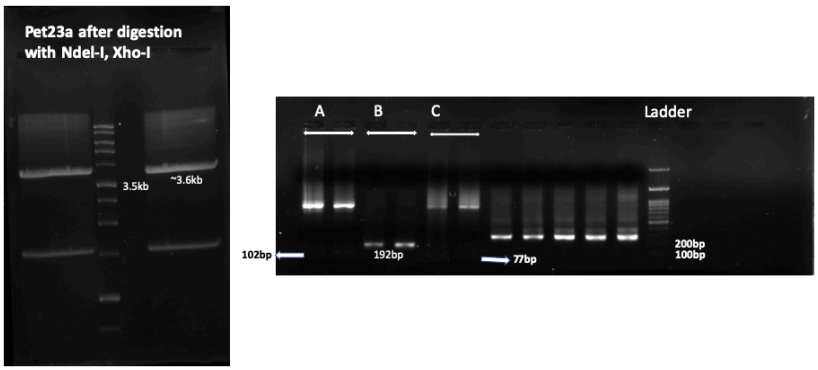

Figure 5 : Restriction Digestion (left) and PCR results (Right)

Double digested pET23a (3.6 kb) (left) and Fragments with respected sizes were observed (right).

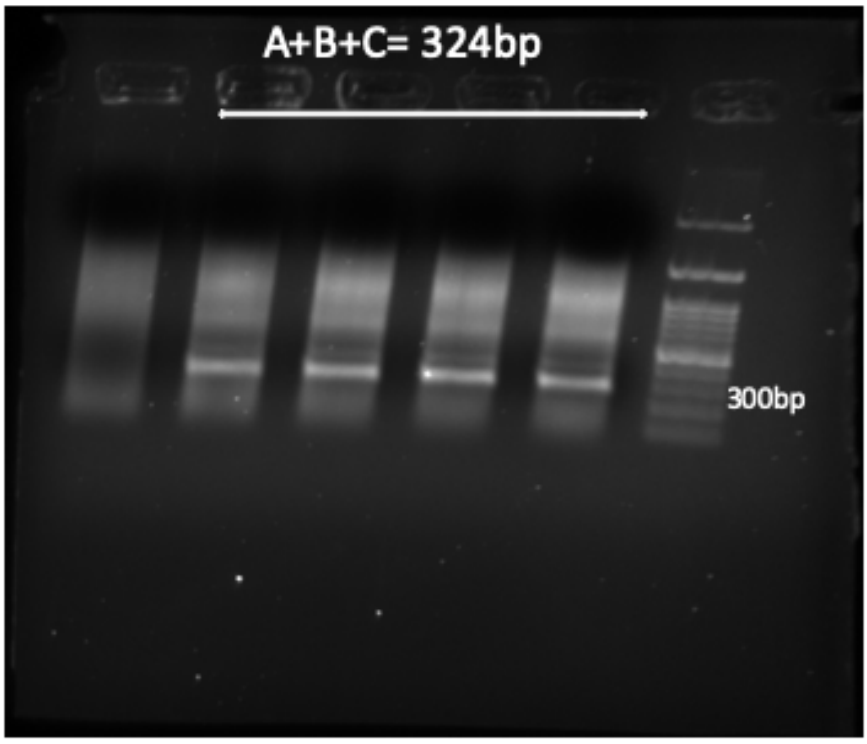

Figure 6 : SOE PCR of A+B+C

A band size of 324 bp (as expected) was observed. Here, a 100 kb ladder was used.

Colony PCR and Restriction digestion

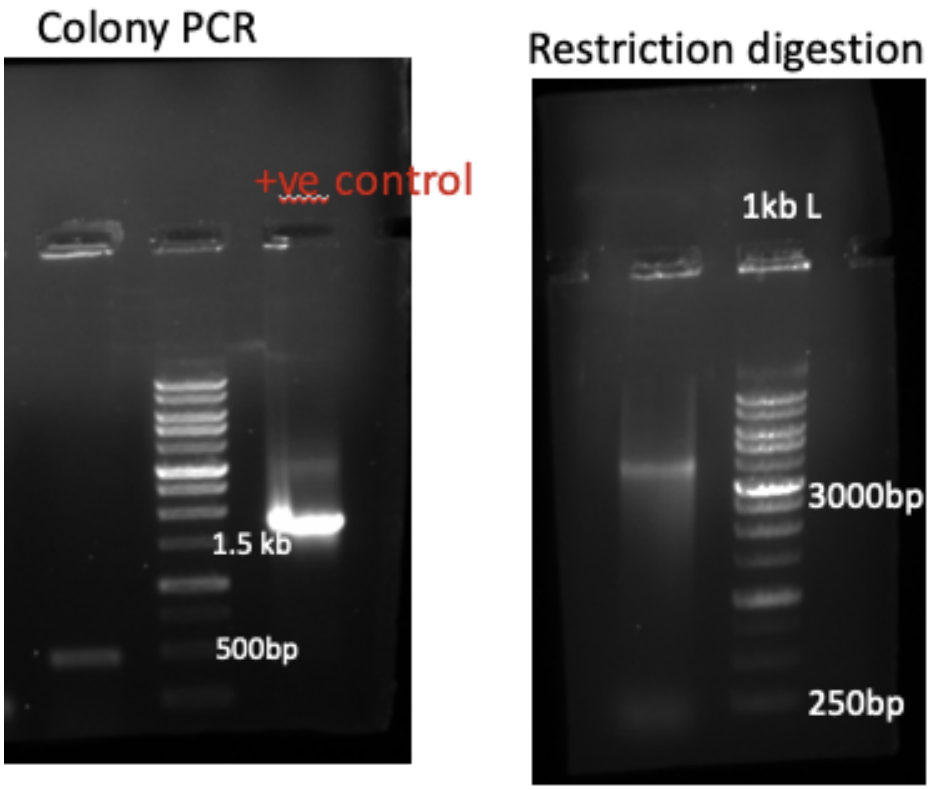

Figure 7 : Colony PCR (lane 1) with a positive control (lane 3) (left) and restriction digestion results (right)

A band size of ~500 bp (as expected with T7 forward and T7 reverse primer) was observed (left) and expected band sizes (~3.6 kb and ~300 bp) after double digestion were also observed. Though the band, which was supposed to come at ~300 bp, came at ~250 bp, we still went ahead with sequencing. Here, a 1 kb ladder was used for both the experiments.

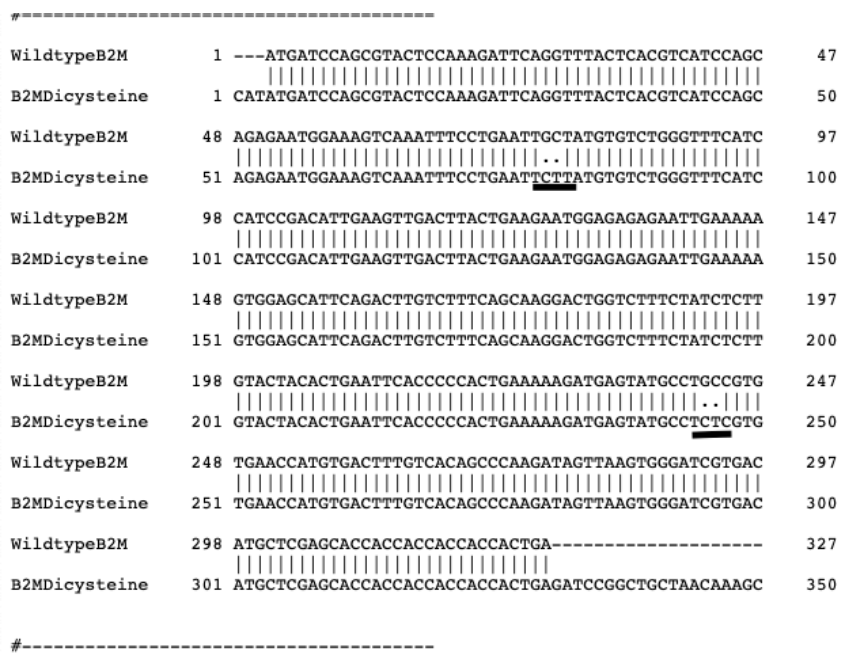

Figure 8 : DNA sequence of di-cysteine mutant aligned against wildtype β_2m.

Expected mutations were observed.

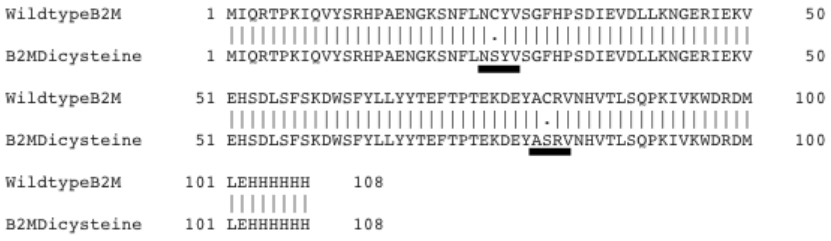

Figure 9 : Protein sequence of di-cysteine mutant aligned against wildtype β_2m.

Expected mutations C→ S at 25th position and 80th position, were observed.

1.3.14 Di-cysteine Mutant (mβ$_2$m) expression and purification

From the transformed plates, 4 colonies were picked and their expression checks were done (Figure 10). From them, the 3rd colony showed a promising induction with a more intense band (in the induced sample) corresponding to mβ$_2$m (11.8 kDa). However, the band was relatively faint as compared to any normal induction. So, we thought that most of the proteins might be going into the inclusion body. Hence, to recover them, we lysed the induced cells in presence of 8 M urea and 6 M GdmCl. We found a better recovery in 8 M urea (Figure 11). So, we carried out a denaturing purification for mβ$_2$m with 8 M urea (same as wildtype).

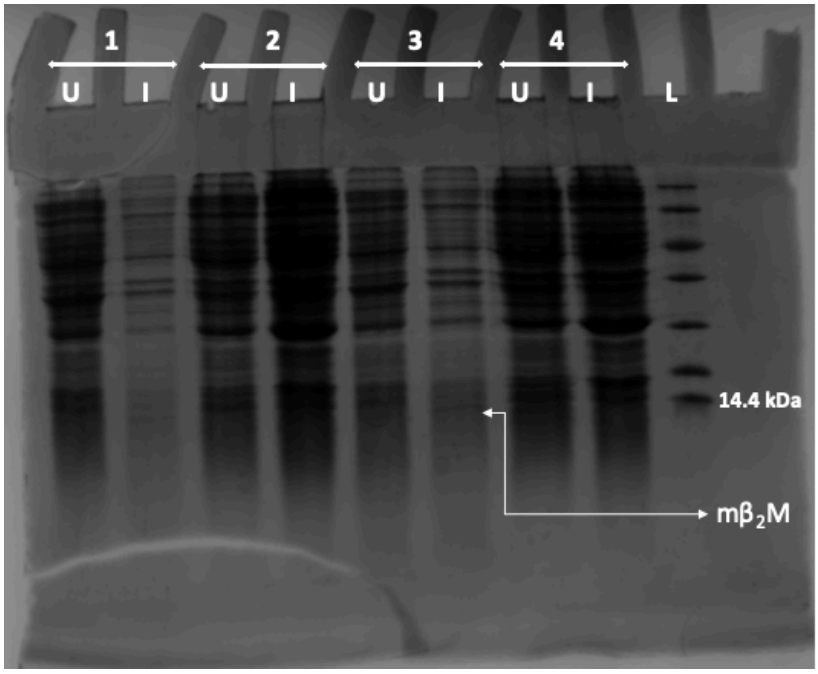

Figure 10 : Expression check of 4 di-cysteine mutant colonies

Colony 3 showed a promising induction.

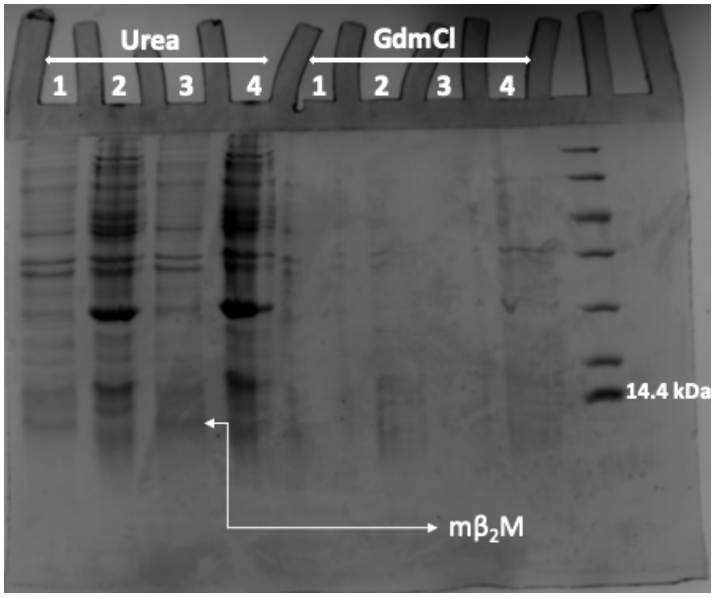

Figure 11 : Recovery of di-cysteine mutated β_2m from the inclusion body.

Most of the mβ_2m was present in the inclusion body, which was successfully recovered with 8 M urea.

Chapter 2

2.1 Results and Discussion

2.1.1 β_2 microglobulin forms oligomers, when it was loaded with non-reducing sample loading buffer in an SDS-PAGE, which got reduced into monomers upon treatment of reducing sample loading buffer

We found β_2 microglobulin forms oligomers when it was loaded with non-reducing sample loading buffer in an SDS-PAGE (we observed oligomers till trimers) (Figure 12, lane 8). Upon treating the sample with reducing sample loading buffer, these oligomers dissociated into monomers (Figure 12, lane 7), indicating that the intermolecular disulfide bonds might be responsible for its oligomerization. In order to further confirm this result, we investigated the competence of di-cysteine mutants to undergo oligomerization.

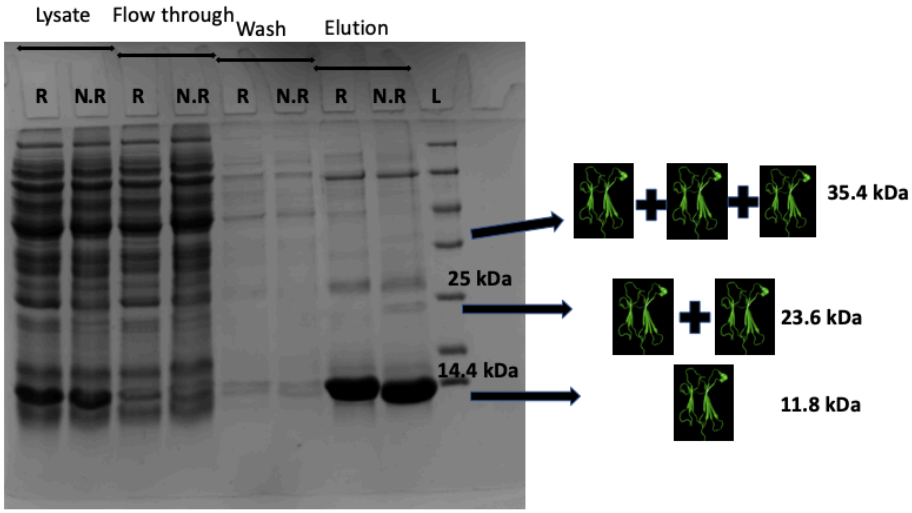

Figure 12 : Oligomerization of β_2m observed with non-reducing sample loading buffer.

Here L denotes Protein ladder, R and N.R represents reducing and non -reducing sample loading buffer respectively. Other unexpected bands seen in lane 7 and 8 are contaminants

2.1.2 The incompetence of di-cysteine mutants to form oligomers confirmed the involvement of intermolecular disulfide bond in β_2m's oligomerization

β_2 microglobulin has two cysteine residues (Figure 2). We mutated them into serine to check its effect on oligomerization. We found that di-cysteine mutants didn't show any oligomers (Figure 13, lane 5), which confirmed that the intermolecular disulfide bond was responsible for the β_2m's oligomerization.

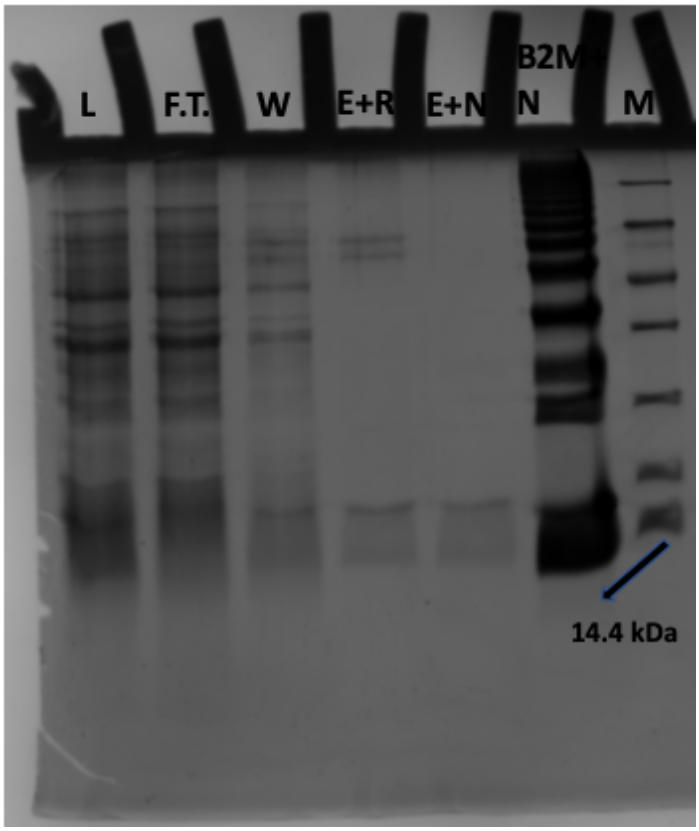

Figure 13 : Oligomerization of di-cysteine mutant

Here M denotes Protein marker, R and N represents reducing and non -reducing sample loading buffer respectively. L, F.T., W, E denotes Lysate, Flow through, Wash, Elution. Lane 6 has denatured β_2m with non-reducing loading buffer, which was added for comparison. Two unexpected extra bands seen at the top (lane 4) with reducing loading buffer, are probably contaminants.

2.1.3 β_2m showed a profound increment in intensity and number of higher-order oligomer when it was purified in denaturing conditions in presence of 8 M urea

We next hypothesized that due to the burial of cysteines in β_2m's native structure (Figure 2), we were not able to observe any higher-order oligomers. Hence, in order to enhance the propensity of formation of the intermolecular disulfide bonds, we decided to carry out the purification under denaturing conditions (with 8 M urea), so as to expose the buried cysteines. As expected, we found a profound increment in intensity and number of higher-order oligomers (Figure 14, Lane 9). In fact, we observed oligomerization till dodecamers. We propose that these newly formed oligomers could be used as a protein marker for SDS-PAGE analysis.

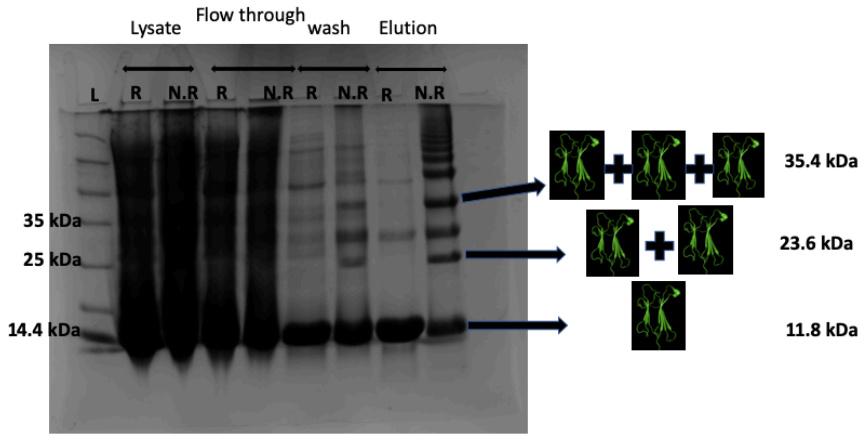

Figure 14 : Oligomerization of denatured β_2m

Here L denotes Protein ladder, R and N.R represents reducing and non -reducing sample loading buffer respectively. Two unexpected extra bands seen in lane 8 (near 27 and 45 kDa) are contaminants.

2.1.4 Glutaraldehyde was not able to crosslink β_2m

It is known that an equilibrium always exists between the reactant and the product in a reversible chemical reaction, and the equilibrium can be driven towards the more populated product by stabilizing the formed product. So, we next thought to enrich these higher-order oligomers of β_2m by cross-linking the lower-order oligomers with glutaraldehyde, which would lock the formed oligomers and shift the equilibrium towards more populated lower-order oligomers (Monomer ⟹ Lower order oligomer), which would, in turn, increase the probability of molecular collision between them to form higher-order structures (Lower order oligomer ⟹ Higher-order oligomer). So, we incubated β_2m (in 8 M urea) with glutaraldehyde for 30 minutes and loaded them with non-reducing sample loading buffer in an SDS-PAGE. But, we didn't observe any increment either in intensity or in the number of higher-order oligomers (Figure 15, Lane 4 and 5). Hence, to check glutaraldehyde's cross-linking ability on β_2m, we incubated already formed oligomers with glutaraldehyde and ran them with reducing sample loading buffer in an SDS-PAGE. Surprisingly, we found that they all got reduced into monomer (Figure 15, lane 7), indicating glutaraldehyde wasn't able to cross-link β_2m.

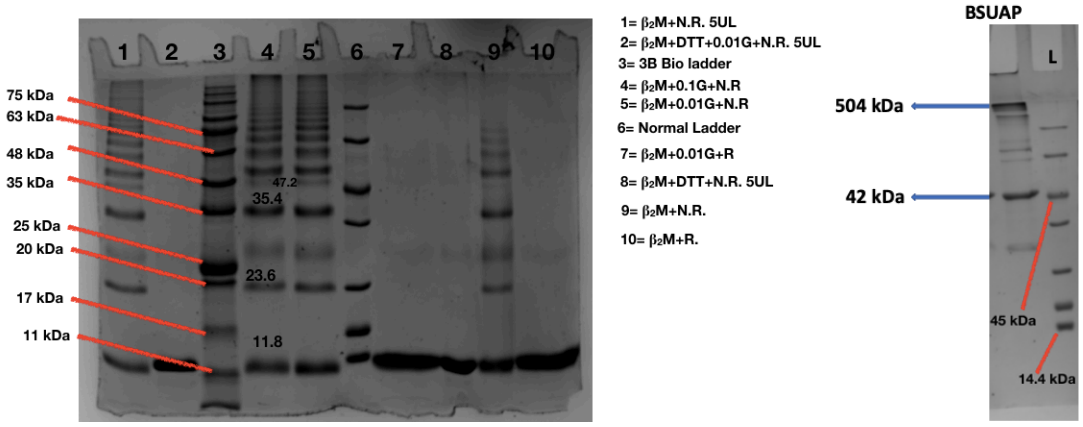

Figure 15 : Glutaraldehyde cross-linking of β_2m oligomers

Here, R and N.R represents reducing and non -reducing sample loading buffer respectively. G denotes glutaraldehyde in % and L (right) denotes protein ladder. β_2m concentration was 0.5 mg/ml. BsuAP, which forms SDS sensitive dodecamers (504 kDa) used as +ve control (right).

2.1.5 The oligomers are forming just after the lysis of BL-21 cells

We next planned to track the oligomer formation during denaturing purification. To check the presence of oligomers inside the cell, we boiled the over-expressed BL21 cells with SDS and ran them with non-reducing SDS-PAGE loading buffer. As expected, due to the reducing environment of the cells, we didn't observe any oligomers (Figure 16, Lane 2). Next, in order to check the presence of oligomers in the cell lysis buffer (8 M urea, pH 8.0), we carried out an on-column refolding (OCR) purification and ran the lysate, flow-through, wash, and elute with non-reducing SDS-PAGE buffer. We observed β_2m oligomers in the lysate, flow-through, and elute, suggesting an aerial oxidation after the lysis of the cells (Figure 17, Lane 2,5,9). Together, these results indicate that β_2m oligomers are forming just after the lysis of BL21 cells in 8 M urea.

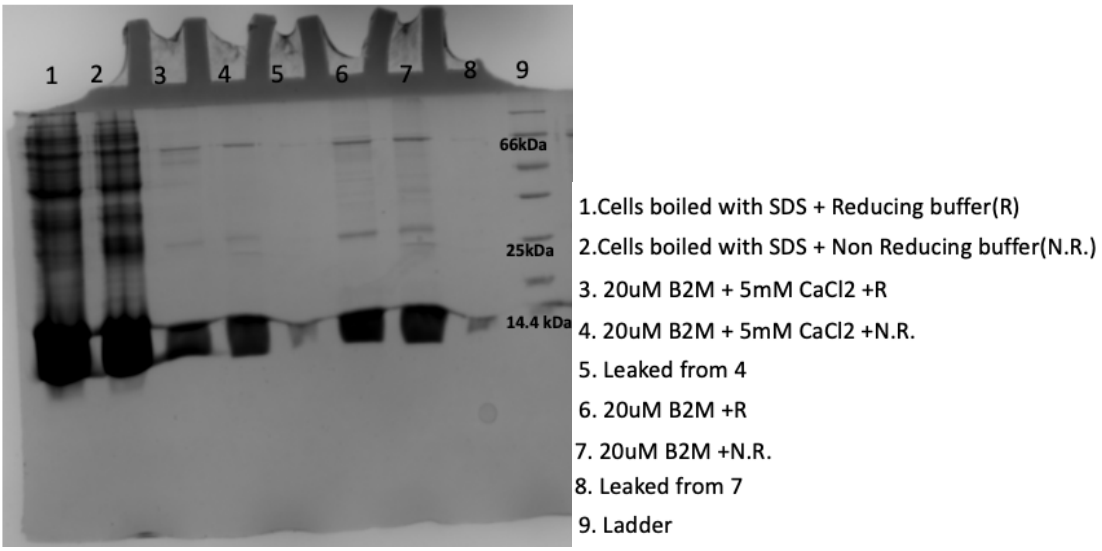

Figure 16 : Presence of β_2m oligomers inside BL21 cells.

Extra unexpected bands seen at the top of 25 kDa in lane 1,2,3,4,6,7 are contaminants.

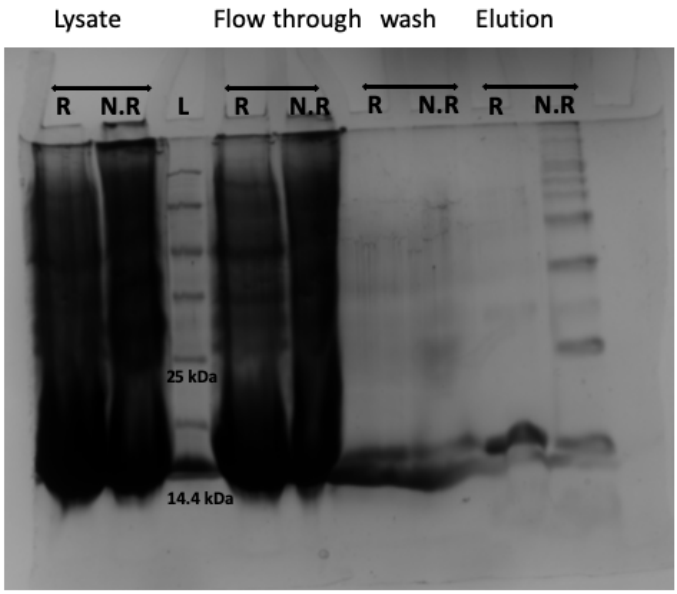

Figure 17 : Initiation of oligomerization during on-column refolding.

Here, R and N.R represents reducing and non -reducing sample loading buffer respectively and L denotes protein ladder.

2.1.6 Characterization of Ca^{2+} induced oligomers

In a different study, our lab has shown that β_2 microglobulin forms amorphous aggregates in presence of Ca^{2+}, which, if incubated for 3-4 weeks, gets converted into amyloid aggregates. We next set out to characterize these Ca^{2+} induced oligomers. So, we asked: Are these Ca^{2+} induced oligomers disulfide-linked? In other words, is Ca^{2+} enhancing these disulfide-linked oligomers?

2.1.6.1 SDS-PAGE analysis revealed that Ca^{2+} induced oligomers are totally different from disulfide-linked oligomers

We ran these Ca^{2+} induced amorphous aggregates with non-reducing sample loading buffer in an SDS-PAGE. However, the SDS-PAGE analysis revealed a single band corresponding to monomer, indicating a totally different nature of these Ca^{2+} induced oligomers (Figure 16, Lane 3).

2.1.6.2 Ca^{2+} induced structural changes don't affect the microenvironment of tryptophan residues

In order to further characterize these Ca^{2+} induced oligomers, we next directed our efforts to monitor changes in intrinsic tryptophan fluorescence upon binding to Ca^{2+}. β_2m has two tryptophan, one exposed (W60) and other partially buried (W95) (Figure 2) (Trinh CH, 2002). The steady-state tryptophan fluorescence measurements, both in presence and absence of Ca^{2+}, showed a peak at ~342 nm that corresponds to partially buried tryptophan, indicating Ca^{2+} induced structural changes don't affect the microenvironment of tryptophan residues (Figure 18).

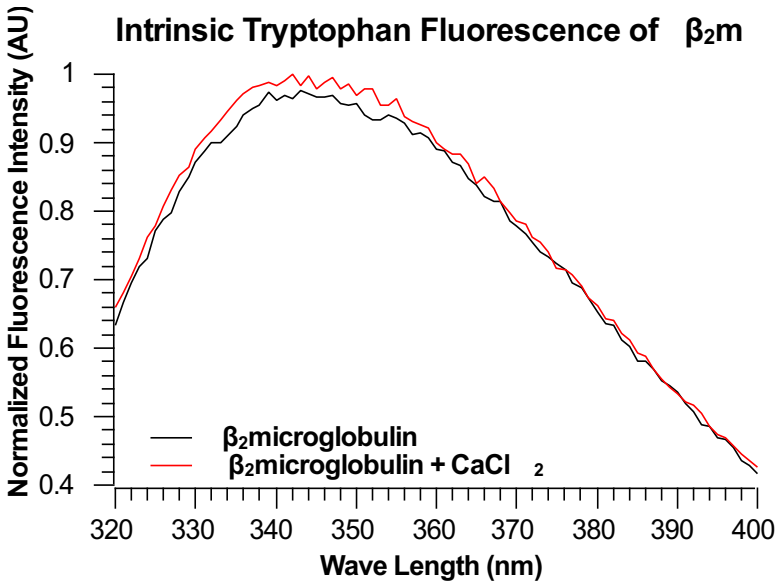

Figure 18 : Intrinsic tryptophan fluorescence of β_2m in presence and absence of $CaCl_2$.

This graph is drawn using scidavis.

2.1.6.3 ANS binding revealed exposure of some hydrophobic patches upon Ca^{2+} binding

Since β_2m contains some hydrophobic patches in its native structure (Figure 2), we next investigated the conformational changes induced by Ca^{2+}, using ANS, which fluoresces strongly upon binding to the hydrophobic environment (Semisotnov GV, 1991). We observed a slight increase in the ANS fluorescence in presence of Ca^{2+},

indicating exposure of some hydrophobic patches upon Ca^{2+} binding (Figure 19). We propose that β strand E, being the most hydrophobic and present close to a predicted Ca^{2+} binding site EKD (74-76) (Kumar S., 2014), shows some dynamics upon binding to Ca^{2+}, which probably initiates Ca^{2+} induced self-assembly of β_2m.

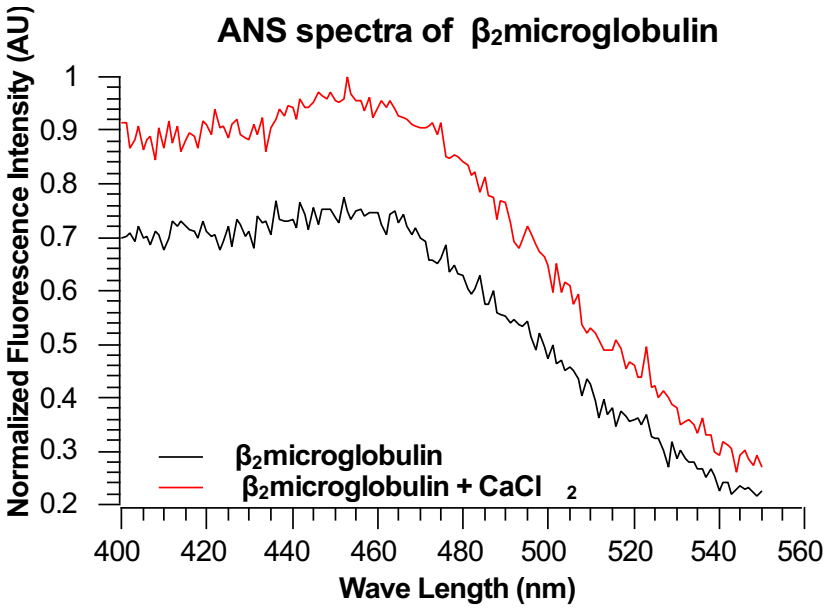

Figure 19 : ANS emission spectra in presence and absence of $CaCl_2$.

This graph is drawn using scidavis.

2.1.6.4 Intrinsic blue fluorescence measurements showed Ca^{2+} binding doesn't affect the intermolecular charge transfer through the hydrogen-bonded networks of the polypeptide backbone

It has been known that an intrinsic blue fluorescence arises due to an extensive intermolecular charge transfer through the hydrogen-bonded networks of the polypeptide backbone (Shukla, et al., 2004) (Del Mercato, et al., 2007) (Pinotsi, et al., 2016) (Prasad, et al., 2017) (Sharpe, Simonetti, Yau, & Walsh, 2011). We found that β_2m, at a concentration of 51 μM, shows an intrinsic blue fluorescence (peaked at ~399 nm), when excited at 310 nm. In order to further check if Ca^{2+} binding is affecting this intermolecular charge transfer, we monitored intrinsic blue fluorescence in presence of Ca^{2+}. However, we didn't observe any significant changes, indicating

Ca^{2+} binding doesn't affect the intermolecular charge transfer through the hydrogen-bonded networks of the polypeptide backbone. (Figure 20).

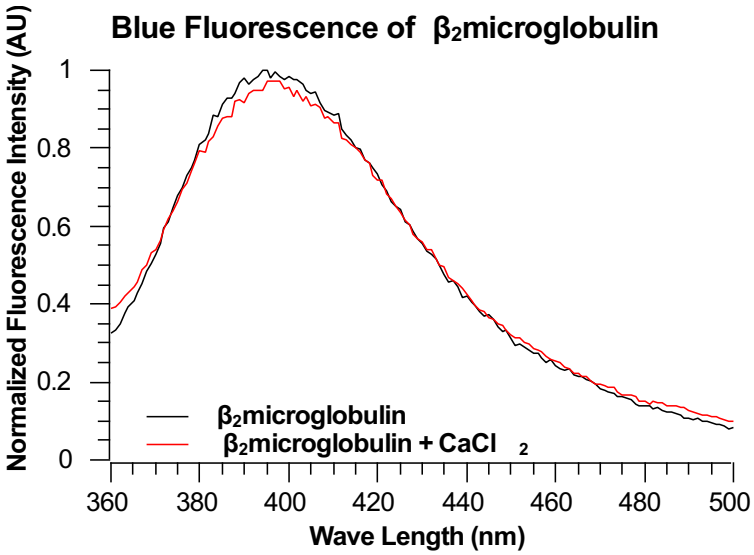

Figure 20 : Intrinsic blue fluorescence of β_2m in presence and absence of $CaCl_2$.

This graph is drawn using scidavis.

2.1.7 Ca^{2+} induced oligomers of β_2m don't undergo LLPS on its pathway to amorphous aggregates

A growing body of intense current research has revealed that a lot of proteins phase separate into liquid condensates before they precipitate into amyloid aggregates. So, to check if Ca^{2+} induced oligomers of β_2m are forming LLPS (Liquid-Liquid Phase Separation), we studied them using confocal microscopy. We observed mesh-like networks, just after the addition of Ca^{2+}, eliminating the involvement of LLPS on β_2m's pathway to amorphous aggregates (Figure 21).

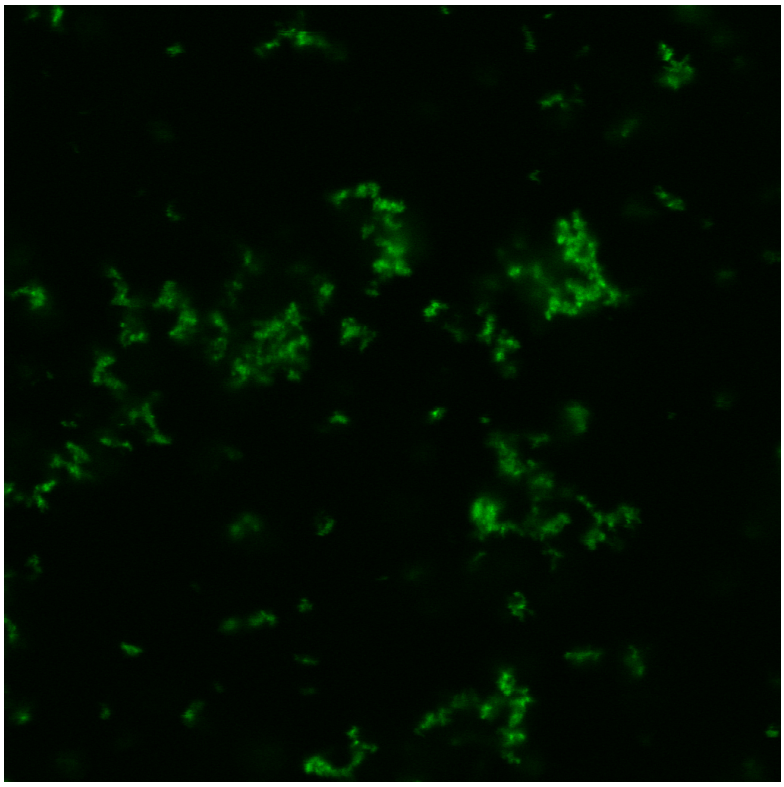

Figure 21 : Confocal images of Ca^{2+} induced aggregates of β_2m

2.2 Conclusions :

In the first part of our study, we found that β_2m forms disulfide-linked oligomers. We enhanced the propensity of formation of these oligomers by exposing the buried cysteines with urea, which caused a profound increment in intensity and number of higher-order oligomers. We propose that these newly formed oligomers could be used as a protein ladder for SDS-PAGE analysis.

In patients suffering from renal dysfunction, β_2m gets aggregated and deposited in the joints, causing carpal tunnel syndrome, amyloid arthropathy, and pathological bone disruption, collectively known as Dialysis Related Amyloidosis (DRA). But, how this aggregation and deposition happens still remains elusive. Guptasarma and colleagues have demonstrated that the physiological concentration of Ca^{2+} causes some conformational changes in β_2m, which drives the protein to precipitate into amorphous forms that later transform into amyloid aggregates. But, they have not commented anything on the molecular mechanism of these conformational changes. So, in the second part of our study, we characterized Ca^{2+} induced oligomers using Intrinsic tryptophan fluorescence, ANS binding, and intrinsic blue fluorescence. We observed a slight increase in the ANS fluorescence in presence of Ca^{2+}, indicating exposure of some hydrophobic patches upon Ca^{2+} binding. We propose that β strand E, being the most hydrophobic and present close to a predicted Ca^{2+} binding site EKD (74-76), shows some dynamics upon binding to Ca^{2+}, which probably initiates Ca^{2+} induced self-assembly of β_2m.

2.3 Future directions:

Further characterization of Ca^{2+} induced oligomers can be done using both far and near UV CD spectra as well as time-resolved ANS binding experiments. It has been known that ΔN6, a variant of β_2m, constitutes ~30 % of β_2m present in amyloid deposits *in vivo* (Linke RP, 1987) (Stoppini M, 2005). Also, it has been shown that ΔN6 alone can self-associate into amyloid fibrils (Jones S, 2003). Hence, the effect of Ca^{2+} on ΔN6 can be investigated. Bellotti and colleagues have also shown some images of *ex vivo* DRA plaques, in which β_2m aggregates are covering the surfaces of collagen I fibrils (Relini, et al., 2006). Thus, studies involving both Ca^{2+} and collagen I can be done in order to check if they act synergistically or independently. Additionally, the effect of collagen I on ΔN6 can be explored.

Bibliography

1. Le Marchand, T et al. (2018). Conformational dynamics in crystals reveal the molecular bases for D76N beta-2 microglobulin aggregation propensity. Nat Commun, 9 (1), 1658.
2. Floege J, et al. (1991). Clearance and synthesis rates of beta2-microglobulin in patients undergoing hemodialy- sis and in normal subjects. J Lab Clin Med, 118, 153–165.
3. Miyata T, et al. (1998). Beta-2 microglobulin in renal disease. J Am Soc Nephrol, 9: 1723–1735.
4. Jürgen Floege,Markus Ketteler. (2001). Beta2-microglobulin-derived amyloidosis: an update. Kidney Int, 59: 164–171.
5. Radford SE, Gosal WS, Platt GW. (2005). Towards an understanding of the structural molecular mechanism of β2-microglobulin amyloid formation *in vitro*. Biochim Biophys Acta, 1753: 51–63.
6. McParland et al. (2000). Partially unfolded states of beta2-microglobulin and amyloid formation *in vitro*. Biochemistry, 39: 8735–8746.
7. Myers SL et al. (2006). A systematic study of the effect of physiological factors on beta2-microglobulin amyloid formation at neutral pH. Biochemistry, 45: 2311–2321.
8. Verdone, G et al. (2002). The solution structure of human beta2-microglobulin reveals the prodromes of its amyloid transition. Protein Sci , 11: 487–499.
9. Eichner T, Radford SE. (2011). Understanding the complex mechanisms of β2-microglobulin amyloid assembly. FEBS J, 278: 3868–3883.
10. Calabrese, M.F., Eakin, C.M., Wang, J.M., Miranker, A.D. (2008). A regulatable switch mediates self-association in an immunoglobulin fold. Nat Struct Mol Biol, 15: 965–971.
11. Hodkinson JP, Radford SE, Ashcroft AE. (2012). The role of conformational flexibility in β2-microglobulin amyloid fibril formation at neutral pH. Rapid Commun Mass Spectrom, 26: 1783–1792.
12. Morgan CJ, Gelfand M, Atreya C, Miranker AD. (2001). Kidney dialysis-associated amyloidosis: a molecular role for copper in fiber formation. J Mol Biol, 309: 339–345.

13. Trinh CH, Smith DP, Kalverda AP, Phillips SE, Radford SE. (2002). Crystal structure of monomeric human beta-2-microglobulin reveals clues to its amyloidogenic properties. Proc Natl Acad Sci USA, 99:9771–9776.
14. Semisotnov GV et al. (1991). Study of the ‘‘molten globule’’ intermediate state in protein folding by a hydrophobic fluores- cent probe. Biopolymers, 31:119–128.
15. Guptasarma, P et al. (2004). A novel UV laser-induced visible blue radiation from protein crystals and aggregates: scattering artifacts or fluorescence transitions of peptide electrons delocalized through hydrogen bonding? Arch. Biochem. Biophys, 428, 144-153.
16. Rinaldi, R et al. (2007). Charge transport and intrinsic fluorescence in amyloid-like fibrils. Proc. Natl. Acad. Sci. U. S. A., 104, 18019-18024.
17. Pinotsi, D et al. (2016). Proton Transfer and Structure-Specific Fluorescence in Hydrogen Bond-Rich Protein Structures. J. Am. Chem. Soc, 138, 3046-3057.
18. Swaminathan, R et al. (2017). Near UV-Visible electronic absorption originating from charged amino acids in a monomeric protein. Chem. Sci, 8, 5416-5433.
19. Sharpe, S., Simonetti, K., Yau, J., & Walsh, P. (2011). Solid-State NMR characterization of autofluorescent fibrils formed by the elastin-derived peptide GVGVAGVG. Biomacromolecules, 12, 1546-155.
20. Linke RP, Hampl H, Bartel-Schwarze S, Eulitz M. (1987). Beta 2-microglobulin, different fragments and polymers thereof in synovial amyloid in long-term hemodialysis. . Biol Chem Hoppe Seyler, 368(2):137-44.
21. Stoppini M, et al. (2005). Proteomics of beta2-microglobulin amyloid fibrils. Biochim Biophys Acta, 1753(1):23-33.
22. Jones S, Smith DP, Radford SE. (2003). Role of the N and C-terminal strands of beta 2-microglobulin in amyloid formation at neutral pH. J Mol Biol, 330(5):935-41.
23. Major Histocompatibility Complexes and Antigen-Presenting Cells . (n.d.). Retrieved from lumenlearning: https://courses.lumenlearning.com/microbiology/chapter/major-histocompatibility-complexes-and-antigen-presenting-cells/
24. Drueke, T. (1998). Dialysis-related amyloidosis. Nephrol Dial Transplant, 13: 58–64.
25. Kumar S., Sharma P., Arora K., Raje M., Guptasarma P. (2014). Calcium binding to beta-2-microglobulin at physiological Ph drives the occurrence of

conformational changes which cause the protein to precipitate into amorphous forms that subsequently transform into amyloid aggregates. PLoS ONE, art. no. e95725.

26. Bellotti, V et al. (2006). Collagen plays an active role in the aggregation of beta2-microglobulin under physiopathological conditions of dialysis-related amyloidosis. J Biol Chem, 281 (24), 16521-9.